

Data Reconciliation of Immersive Heart Inspection*

Liu X.^{1,2} Koppelaar H.¹ Koffijberg H.¹

1. Knowledge Based System, Faculty of Electrical Engineering, Mathematics and Computer Science, Delft University of Technology, the Netherlands.
h.koppelaar@ewi.tudelft.nl, h.koffijberg@ewi.tudelft.nl
2. College of Information Science and Technology, DongHua University, China.
liu@graphics.tudelft.nl, liuxq@dhuh.edu.cn

Bruining N.³ Hamers R.³

3. Thoraxcentre, Department of Cardiology, Erasmus MC, the Netherlands.
n.bruining@erasmusmc.nl
curad@euronet.nl

Abstract – *IVUS images are complicated medical datasets suffering from some artifacts caused by the data acquisition method of immersive heart inspection. Data reconciliation, which removes tracing and tracking uncertainties of these datasets, is an important step for the medical application of remodeling the arteries in virtual reality to aid diagnosing and treating heart diseases. This paper provides an empirical data reconciliation method, which fuses the features of the coronary longitudinal movement with motion compensation model. It explains the distortion of the data set well and provides a method to analyze and reconcile the dataset.*

Keywords: Medical image mining, IVUS data processing, data reconciliation, data fusion, immersive heart inspection, motion compensation.

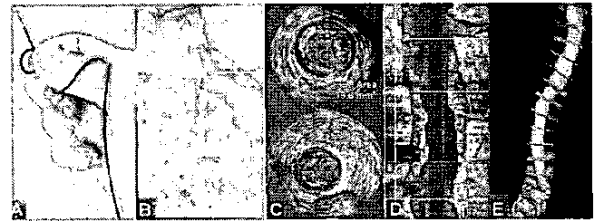
1 Introduction

Heart disease is the leading cause of death in industrialized nations and is characterized by diverse cellular abnormalities associated with decreased ventricular function. Buried within the human body, most knowledge is obtained by autopsy. Live immersive inspection within the human heart requires advanced data acquisition, image mining and virtual reality techniques. Computational sciences are being exploited as means to investigate biomedical processes in cardiology.

1.1 Immersive IVUS heart inspection

To diagnose the possible anomalies and heart diseases is difficult because physicians can't literally see in the human heart. Various data acquisition techniques have been invented to partly remedy the lack of sight: non-invasive inspection including CT (Computerized Tomography), Angiography, MRI (Magnetic Resonance Imaging), ECG signals etc. These techniques do not take into account crucial features of lesion physiology and vascular remodeling to really mine blood-plaque.

Minimal-invasive techniques such as IntraVascular UltraSound (IVUS) provide methods to assess intermediate coronary lesions and also provide guidance both before and after coronary intervention. The IVUS method is invasive, in which a camera is pulled back inside the artery, and the resulting immersive tomographic images are used to remodel the artery. This remodeling of the artery and its virtual reality (VR) aspect offer interesting future alternatives for mining these data to unearth anomalies and diseases in the moving heart and coronary arteries at earlier stage. Figure 1 explains some aspects of IVUS technology.



A: IVUS catheter/endosonics camera and its wire. B: angiography of a contrast-filled section of coronary artery, i.e. the camera's path. C: two IVUS cross-sectional (radial) images and some quantitative measurements on them. D: Virtual longitudinal (axial) view of the vessel reconstruction. E: Virtual 3D-Impression of the vessel reconstruction.

Figure 1. IVUS's inspection camera, its path and its output

IVUS is becoming an important clinical tool in cardiology. It also serves in clinical trials to evaluate results of novel interventional techniques, e.g. local nano-technology pharmaceutical treatments.

1.2 A data reconciliation problem

The IVUS sources are voluminous separated slice images with artifacts generated from the immersive data acquisition procedure [1]:

* 0-7803-8566-7/04/\$20.00 © 2004 IEEE.

1. Ring-down, blood speckle, and near field artifacts.
2. Non-uniform rotational distortion and motion artifacts.
3. Obliquity, eccentricity, and problems of vessel curvature.
4. Problems of spatial orientation (axial positions and orientation of the slices).

These artifacts are generated by the pumping heart, the respiring lung and the moving immersed catheter camera. The first three types are remedied by image processing and therefore fall outside the scope of this paper. For the last type, axial positions are most important. Once the correct positions are found, the orientation can be gained based on the vessel shape by Frenet-Serret theory [16].

Figure 2 explains the longitudinal displacement (in axial z-position) caused by cardiac cycles during a camera pullback in a coronary artery segment. Over 5mm of distortion of the longitudinal catheter motion relative to the coronary vessel may occur during one cardiac cycle, with steady catheter pull-back at 0.5 mm/sec (curve D of Fig. 2), the non-gated samples (curve F dot points of Fig. 2) were stored on S-VHS videotape at a rate of 25 images/sec [2]. The catheter position equals the sum of the pullback distance and the longitudinal catheter displacement. In F, the absolute catheter positions of solid dots are in disorder, which will cause a disordered sequence of camera images. The consecutive image samples selected in relation to the positions of the catheter relative to the coronary vessel wall are highlighted in G. In conclusion, these samples used for analysis are anatomically dispersed in space (III, I, V, II, IV, and VI).

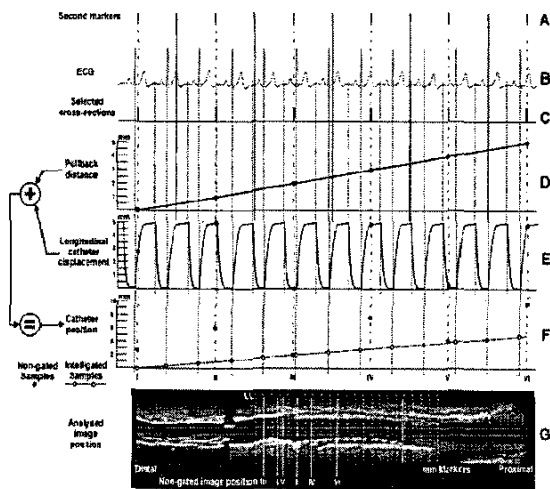


Figure 2. Trajectory position anomalies of the camera

Data reconciliation to cure the anomalies is an important step for medical application of these datasets

and it inspires interdisciplinary work in medicine, physics and computer science.

2 Approaches to data reconciliation

To battle the data reconciliation problem, three types of methods apply: parsimonious data acquisition, fusion of invasive and non-invasive data, and empirical hybrid motion compensation.

2.1 Parsimonious data acquisition

Cardiac knowledge dictates systolic/diastolic timing features. IVUS images are recorded in the end-diastolic phase of the cardiac cycle, in which the heart is motionless and the blood flow has ceased so that their influences on the catheter can be neglected. Online ECG-gated pullback has been used to acquire phase-dependent data, but the technology is expensive and prolongs the acquisition procedure. Instead, a retrospective image-based gating mining method has been studied [2], [3]. In this method, the different features are mined from sampled IVUS images over time by transforming the data with spectral analysis, to discover the most prominent repetition frequencies of appearance of these image features. From this the near images at the end-diastolic phase can be inferred. The selection of images is parsimonious: only about 5% of the dataset is sampled, wherein about 10% of the selected images are mispositioned. Computational costs is also a disadvantage of this method, a supercomputer has been built to mine these data [4].

2.2 Data fusion

The motion artery courses provide helpful information to identify space and time of the IVUS camera in the coronary of the moving heart. Fusion of complementary information from two or more differing modalities enhances insights into the underlying anatomy and physiology. Combining non-invasive data mining techniques to battle measurement errors is a preferred method. The positioning for the camera could be remedied if from angiograms the outer form of an artery is available, as a path-road for the camera. Fusing the route and IVUS data, a simulator generates a VR reconstruction of the vessel [6-10]. This should help to estimate the absolute catheter spatial positions and orientations, but usually the routes are static and data are parsimonious, phase-dependent, or without exhibiting the distortion.

2.3 Hybrid motion compensation

Physical prior knowledge could predict space and time of the global position of IVUS camera, if it would be fully modeled. The many mechanical and electrical mechanisms in a heart make a full model intractable, but if most of its mechanisms could be dispensed with, the prediction model would become considerably simplified.

There are few papers on consecutive motion tracking (3D plus time) of the coronary tree [12, 13], but they omitted the axial stretch of the arteries, which is the most important property for accurate positioning analyses. In order to gain further analysis and application of the immersive IVUS data, this paper discusses a hybrid motion compensation method to improve longitudinal data reconciliation, which fuses the empirical longitudinal deformation model from the angiograms of the artery.

3 Hybrid longitudinal motion compensation

In order to set up the motion compensation model, we need to consider the physical factors influence on axial data distortion:

- Heart movement (compression/expansion): Causes the artery to stretch.
- Respiration: Causes artery and catheter to move together, but the relative movement between them is small, mainly on camera rotation.
- Heart blood pulse: Causes the artery to stretch but smaller to compare with heart movement.
- Catheter pullback: The camera moves relative to the inside of the artery through steady pullback.

The main longitudinal data distortion is caused by the artery deformation due to the periodic compression and expansion of the heart. The movement between the camera and the artery is simplified by the following reasonable hypotheses:

- The blood pulse is negligible and is not considered.
- The arteries are thought to be curved tubes, which undergo longitudinal deformations.
- The vessel wall is locally orthogonal, anisotropic, elastic and incompressible.
- The camera is pulled back steadily along the artery centerline.
- The angiograms in one cardiac cycle are taken under breath-hold situation and the respiration is not considered.

3.1 Data sets acquisition and organization

Cineangiogram provides a series of 2D projected images (from 2 projection angles) of the moving heart (15~30 frames/sec) under breath-hold. Semiautomatic 3D reconstruction of the 2D projected images provides 3D coordinates of the artery central line [5]. The 3D coordinate data sets in one cardiac cycle are recorded.

The axial motions of individual section of the coronary arteries are different. This is due to anisotropy of heart motion. So small segments sampled of artery sections and a bio-model data organization for the

coronary artery tree will be better. But very fine-grained sampling, point-to-point of the artery cannot be achieved directly from cineangiogram sequences. Marking all the special points such as bifurcations, proximal and fixed points to segment the arteries, the reconstructed coronary arterial tree is represented by a hierarchical digraph or a linked multi-tree data structure [14] illustrated in Figure 3 (breadth). Each pair of adjacent nodes represent an artery segment, which is denoted by c_{mn} , $0 \leq m, n \leq pnum - 1$, $pnum$ counts the special points. The 3D artery centerline coordinate points, sampled along the segment length, are $c_{mn} = P^{mn} = \{p_0^{mn}, p_1^{mn}, \dots, p_{k_{mn}-1}^{mn}\} \in R^3$, k_{mn} counts the sampled points on the artery segment. The coronary tree is a set $T = \{c_{mn} \mid 0 \leq m, n \leq pnum, d_{mn} \notin \phi\}$, d_{mn} is the edge connected to the special points $p_m, p_n \cdot c_{(mn, ft)}$ with integer ft , $1 \leq ft \leq ftnum$ is a centerline of the segment c_n gained from the angiogram frames at cardiac time phase ft . $ftnum$ counts the angiogram samples in one cardiac cycle.

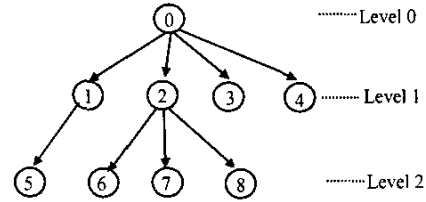


Figure 3. The artery hierarchical digraph

3.2 Artery segment shape acquisition

The segmented hierarchical data-structure organization is employed to store the artery features in one cardiac cycle. In order to get the shapes of the segment arteries and to calculate the features of longitudinal stretch and curvature, also to reduce the storage and save post processing time, the discrete representation of the artery centerlines are converted to parametric representation. Spatial B-Splines [15] provide intrinsic smoothness to the 3D artery curves.

Let $C_{mn}(u) = (x_{mn}(u), y_{mn}(u), z_{mn}(u) \mid u \in [0,1])$ be the approximation splines curve of the segment c_{mn} , at time ft using a chord length parameterization of c_{mn} . Cubic B-Splines are used for all artery segments and C^0 continuity is kept at the special points. Then

$$C_{mn}(u) = \sum_{i=0}^{k_{mn}-1} B_i(u) P_i^{mn} \quad (1)$$

$$U_{mn} = \{0,0,0,0, u_4, \dots, u_{k_{mn}-4}, 1,1,1,1\}$$

$\{P_i^{mn}\} \in R^3$ are the k_{mn} control points, and the $\{B_i\}$ are the 3rd degree B-Splines basis functions. U_{mn} is the non-uniform knot vector with length $k_{mn} + 5$. The values at the ends of the curve are constrained to make :

$$\begin{aligned} C_{mn}(0) &= P_0^{mn} \in c_{mn} \\ C_{mn}(1) &= P_{k_{mn}-1}^{mn} \in c_{mn} \end{aligned} \quad (2)$$

In order to keep the adjacent segment to share a control point, force:

$$C_{mn}(1) = C_{rs}(0) \quad \text{if} \quad p_{k_{mn}-1}^{mn} = P_0^{rs} \quad (3)$$

Figure 4 shows an artery branch (c0-2-7-11) with 3 segments (c0-2, c2-7, c7-11) and their shape deformations described by B-Splines in one cardiac cycle (20 sampled curves).

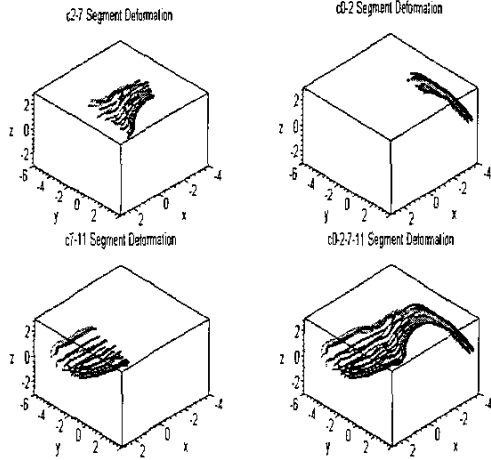


Figure 4. Artery segments shape deformations

3.3 Artery consecutive stretch model

The features of length of every artery segments are calculated from the B-Splines curves. The length L_{mn} of the arterial segment $C_{mn}(u)$ is calculated over the parametric interval $[0,1]$ by formula (4):

$$L_{mn} = \int_0^1 \|C_{mn}'(u)\| du \quad (4)$$

The heart is beating during acquisition of angiograms and IVUS immersive inspection. Therefore, the length stretch dynamics require a time parameter, $C_{mn}(u, ft) = (x_{mn}(u, ft), y_{mn}(u, ft), z_{mn}(u, ft))$, ft is the frame time (phase) of the angiogram in one cardiac cycle.

The arc-length at ft with the same Hölder norm for the time-varied position is described by formula (5):

$$L_{(mn,ft)} = \int_0^1 \|C_{mn}'(u, ft)\| du \quad (5)$$

Assume the longitudinal stretch is uniform on the same segment, so the longitudinal amplitude change can be described by the change of the elasticity ratio relative to the first phase of the artery, for the segment c_{mn} , it is:

$$V_{(mn,ft)} = \frac{L_{(mn,ft)} - L_{(mn,1)}}{L_{(mn,1)}} \quad (6)$$

The longitudinal elasticity ratio $V_{(mn,ft)}$ generated from the angiogram frames is discrete. Consecutive stretch models are needed for immersive camera positions evaluation, since the camera pullback continues and the cycle of the heartbeat is variable.

$$V_{mn}(t) \sim V_{(mn,ft)} \quad (7)$$

Fourier expression is used to model the cyclic elasticity ratio $V_{(mn,ft)}$. The heart's beat is periodical, with intervals in the mean $T = 2\pi / \omega$. T is the cardiac cycle time, ω is the cardiac frequency. The angiogram frames are taken at the equal intervals. The empirical longitudinal elasticity ratio that simulates the stretch caused by artery deformation is in formula (8). It is parameterized by a function approximation resulting in formula (6) $V_{(mn,ft)}$.

$$V_{mn}(t) = a_0 + \sum_{j=1}^J a_j \sin(j\omega t) + b_j \cos(j\omega t) \quad (8)$$

3.4 Hybrid motion compensation

As we discussed in 3.1, in the motion compensation of the camera, we only need to consider the deformed artery length and the momentary pull back length to compensate for the longitudinal motion displacement. For axial motion compensation along artery length, the camera should be at the following wanted artery position $l_w(t)$ at time t , and then the images are in correct order:

$$l_w(t) = l_l - v_c t + \sum_{mn \in B_L} V_{mn}(t) L_{(mn,1)} + V_{m'n'}(t) L_{L(m'n')}(t) \quad (9)$$

$$L_{L(m'n')}(t) = l_l - v_c t - \sum_{mn \in B_L} L_{(mn,1)} \quad (10)$$

B_L is the left catheter route along the branches of the artery tree from the root, for example: if a catheter is pulled back along the route $B = \{0-2,2-7,7-11\}$, and the camera is at the segment c_{7-11} , then $B_L = \{0-2,2-7\}$. $L_{(mn,1)}$ is the initial length of the artery segment c_{mn} at its first angiogram frame. v_c is the camera pullback speed. $V_{mn}(t)$ is the empirically longitudinal elasticity ratio at segment c_{mn} that simulates the longitudinal stretch. l_j is the catheter's initial position (initial length of the whole artery branch as the route of the camera). $c \dots$ is the current segment where the camera is located, $L_{L(m'n')}(t)$ is the left length to be pulled back along $c \dots$.

Data reconciliation is carried out by mapping the camera's wanted position $l_w(t)$ to the length of the first phase of the artery, at every cardiac cycle. Thus we get the relative positions of the image slices on the artery $l_p(t)$, and the sequence of the images can be gained from (11).

$$l_p(t) = \frac{(l_j - v_c t)^2}{l_w(t)} \quad (11)$$

4 Experiment and results

We use the hybrid longitudinal motion compensation method on a segment of the right coronary artery, a branch of the artery tree. In this experiment, the maximum longitudinal stretch is about 10%, which is consistent with the report of 11% length stretch in ascending aorta and pulmonary arteries [11] and nearly 8% length stretch [8] in the left anterior descending aorta; the maximum distance error between two slices is about 2.5mm in one cardiac cycle.

For reading convenience, we assume the cardiac cycle time T to equal 1 second in the following calculation. Figure 5 shows the longitudinal stretch of a segment in one cardiac cycle. Figure 6 shows the empirical longitudinal elasticity ratio of a segment, $V_{mn}(t)$ is parameterized by $J = 6$.

Figure 7 shows the relative positions of the camera and the image slices, according to the empirical motion compensation in one cardiac cycle. In figure 7, a camera is pulled back at the speed of 0.05mm/s, and it is experiencing a new heart cycle starting at the position of 2.75mm relative to the artery root. Ten camera position samples c_i are chosen. In order to maintain the ordering, the camera should be at positions along the curve where w_i is depicted (camera's wanted positions). After data reconciliation, the images' positions on the artery are depicted by the p_i along the coordinate length axis.

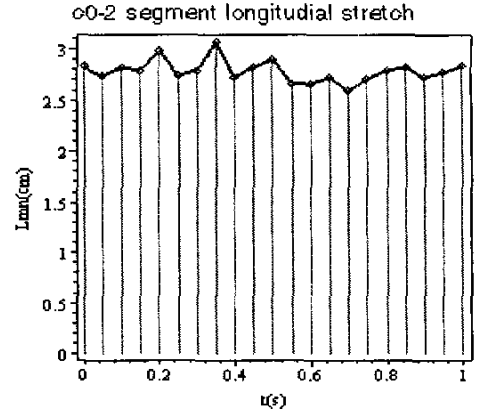


Figure 5. The longitudinal stretch of a segment

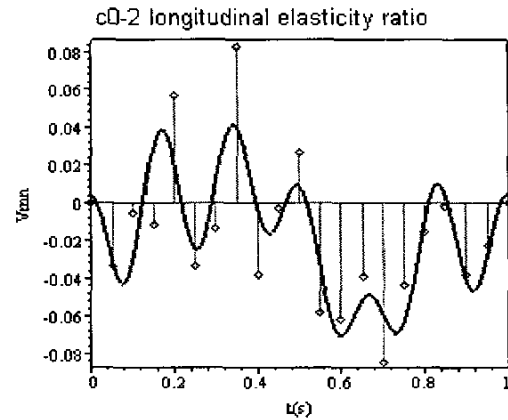


Figure 6. Empirical longitudinal elasticity ratio model
Motion compensation and camera positions

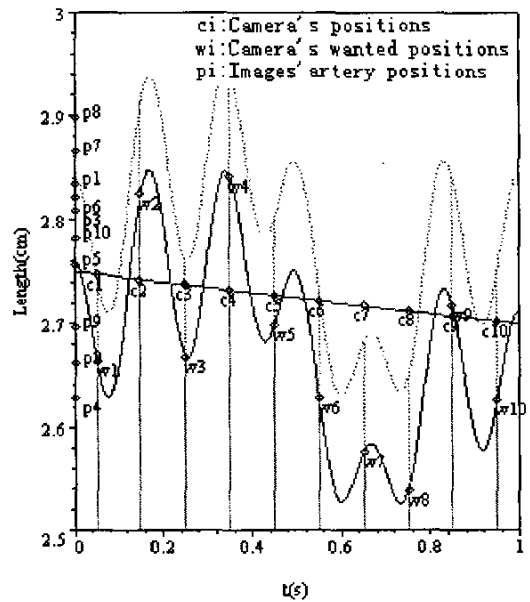


Figure 7. Motion compensation and the camera positions

5 Conclusion

Fusing the empirical features of the coronary longitudinal movement with our motion compensation model is a way to resolve the longitudinal distortion of the IVUS dataset. It explains the distortion of the dataset well and repairs the dataset.

We did not evaluate data from patients with implants. Statistical experiments may find the non-isometric stretch governing in different parts of the coronary arteries to also help evaluating the stenosed segments. Accurate 3D positions are important for this method. For more accurate position analysis, some other related factors need to be considered, for example, the catheter tube may be displaced from the artery centerline. And the heart, which functions like a suction pump, could have jerky motions that may deviate from the general one cycle route.

References

- [1] Mintz, G. S., Nissen, S. E., Anderson, W. D., Bailey, S. R., Erbel, R., Fitzgerald, P. J., Pinto, F. J., Rosenfield, K., Siegel, R. J., Tuzcu, E. M., and Yock, P. G., "ACC clinical expert consensus document on standards for the acquisition, measurement and reporting of intravascular ultrasound studies", *Journal of the American College of Cardiology*, Vol. 37, pp. 1478-1492, 2001.
- [2] Winter, S. A. de, Hamers, R., Degertekin, M., Tanabe, K., Lemos, P.A., Serruys, P.W., Roelandt, J. R. T. C., and Bruining, N., "Retrospective image-based gating of intracoronary ultrasound images for improved quantitative analysis: the intelligate method", *Catheterization and Cardiovascular Interventions*, Vol. 61, No 1, pp. 84 -94, 2004.
- [3] Zhu, H., Oakeson, K. D., and Friedman, M. H., "Retrieval of cardiac phase from IVUS sequences", William, F. Walker, Michael, F., and Insana (Eds.): *Medical Imaging 2003: Ultrasonic Imaging and Signal Processing*, Proceedings of SPIE 5035, pp. 135-146, 2003.
- [4] Winter, S. A. de, Koppelaar, H., Hamers, R., Degertekin, M., Tanabe, K., Lemos, P., Serruys, P., Roelandt, J., and Bruining, N., "The IntelliGate automated image-based gating algorithm for intracoronary ultrasound images", BNAIC, Nijmegen, the Netherlands, pp. 363-370, 2003.
- [5] Guggenheim, N., Doriot, P. A., Dorsaz, P. A., Descouts, P., Rutishauser, W., "Spatial reconstruction of coronary arteries from angiographic images", *Physics in Medicine Biology*, Vol. 36, pp. 99 -110, 1991.
- [6] Wahle, A., Mitchell, S. C., Olszewski, M. E., Long, R. M., and Sonka, M., "Accurate visualization and quantification of coronary vasculature by 3-D/4-D fusion from biplane angiography and intravascular ultrasound", EBiOS 2000, Biomonitoring and Endoscopy Technologies, Amsterdam NL, SPIE Europto, 4158, pp. 144 -155, 2000.
- [7] Sarry, L. and Boire, J. Y., "Three-Dimensional tracking of coronary arteries from biplane angiographic sequences using parametrically deformationable models", *IEEE Transactions on Medical Imaging*, Vol. 20, No. 12, pp. 1341 - 1351, 2001.
- [8] Ding, Z. and Friedman, M.H., "Quantification of 3D coronary arterial motion using clinical biplane cineangiograms", *The International Journal of Cardiac Imaging*, Vol. 16, No. 5, pp. 331 - 346, 2000.
- [9] Rotger, B., Radeva, P., Mauri, J., and Fernandez-Nofrerias, E., "Internal and external coronary vessel images registration", Escrig, M. T., Toledo, F., and Golobardes, E. (Eds.): *Topics in Artificial Intelligence*, 5th Catalanian Conference on AI, CCIA 2002, Castellón, Spain, pp. 408 - 418, October, 2002.
- [10] Weichert, F., Wawro, M., and Wilke, C., "A 3D computer graphics approach to brachytherapy planning", *The International Journal of Cardiovascular Imaging*, Vol. 20, pp. 173 - 182, 2004.
- [11] Patel, D. J. and Fry, D. L. "In situ pressure-radius-length measurements in ascending aorta of anesthetized dogs", *Journal of Applied Physiology*, Vol. 19, pp. 413 - 416, 1964.
- [12] Chen, S-Y. J. and Carroll, J. D., "Kinematic and deformation analysis of 4-D coronary arterial trees reconstructed from cine angiograms", *IEEE Transactions on Medical Imaging*, Vol. 22, No. 6, pp. 710 - 720, 2003.
- [13] Shechter, G., Devernay, F., Coste-Maniere, E., Quyyumi, A., and McVeigh, E. R., "Three-Dimensional motion tracking of coronary arteries in biplane", *IEEE Transaction on Medical Imaging*, Vol. 2, pp. 1- 16, 2003.
- [14] Chen, S-Y. J. and Carroll, J. D., "3-D Reconstruction of coronary arterial tree to optimize angiographic visualization", *IEEE Transactions on Medical Imaging*, Vol. 19, No. 4, pp. 318 - 336, 2000.
- [15] Bartels, R. H., Beatty, J. C., and Barsky B. A., *An Introduction to Splines for Use in Computer Graphics & Geometric Modeling*, Morgan Kaufmann Publishers, INC. 1987.
- [16] Millman, R. S. and Parker, G. D., *Elements of Differential Geometry*, Englewood Cliffs, NJ: Prentice-Hall, 1977.